

Transport properties of Metallic Ruthenates: a DFT+DMFT investigation

Xiaoyu Deng,¹ Kristjan Haule,¹ and Gabriel Kotliar¹

¹*Department of Physics and Astronomy, Rutgers University, Piscataway, New Jersey 08854, USA*

(Dated: January 28, 2022)

We present a systematical theoretical study on the transport properties of an archetypal family of Hund's metals, Sr_2RuO_4 , $\text{Sr}_3\text{Ru}_2\text{O}_7$, SrRuO_3 and CaRuO_3 , within the combination of first principles density functional theory and dynamical mean field theory. The agreement between theory and experiments for optical conductivity and resistivity is good, which indicates that electron-electron scattering dominates the transport of ruthenates. We demonstrate that in the single-site dynamical mean field approach the transport properties of Hund's metals fall into the scenario of "resilient quasiparticles". We explain why the single layered compound Sr_2RuO_4 has a relative weak correlation with respect to its siblings, which corroborates its good metallicity.

PACS numbers: 71.27.+a, 72.10.-d, 78.20.-e

The anomalous transport properties in correlated metals have been of great interest for many decades, but the main focus was the electron-electron scattering due to Hubbard-like short range repulsion. Many features found in realistic materials are well captured by the dynamical mean field theory (DMFT) in simple Hubbard models[1, 2], for example, the very low coherence scale T_{FL} below which Fermi liquid (FL) theory holds [3], and the high temperature "bad metal" behavior that resistivity exceeds the Mott-Ioffe-Regel limit[4]. In the broad crossover regime between FL and "bad metal" the "resilient quasiparticles" which survive up to high temperature[5, 6] dominate the transport. Very recently Hund's metals[7] have attracted a lot of attentions. These are materials in which the Hund's interaction rather than the Hubbard repulsion gives rise to the heavy quasiparticle mass in several transition metal compounds such as iron pnictides[8] and ruthenates[9, 10]. The understanding of the scattering mechanism in Hund's metals and their consequences for the transport properties have not been explored much.

In this paper we study the archetypal Hund's metals[9–11], the metallic members of Ruddlesden-Popper series of ruthenates ($\text{A}_{n+1}\text{B}_n\text{O}_{3n+1}$): Sr_2RuO_4 ($n = 1$), $\text{Sr}_3\text{Ru}_2\text{O}_7$ ($n = 2$), SrRuO_3 and CaRuO_3 ($n = \infty$). Ruthenates have been extensively studied as prototypical strongly correlated systems, with large effective mass enhancements revealed by various experiments[12–25]. They exhibit a very small coherence scale T_{FL} , as well as a crossover into "bad metal" regime[25–30]. Surprisingly the single layered compounds Sr_2RuO_4 is more metallic than the pseudocubic SrRuO_3 and CaRuO_3 at relative low temperature ($\leq 400\text{K}$). This is different from many other systems, for example, the Ruddlesden-Popper family of strontium vanadates, lanthanum nickelates, lanthanum cuprates, strontium iridates, where the single layered compounds are insulating and the pseudocubic ones are metallic.

The method used in this paper is the combination of density functional theory and DMFT (DFT+DMFT)

in the charge self-consistent and all electron formulation that avoids building the low energy Hubbard model, which is successful in the quantitative descriptions of electronic structures in many correlated systems[31]. There are a few DFT+DMFT studies on ruthenates available in the literature[9, 32–34] but they are performed on low energy Hubbard models. Moreover a complete investigation of the transport properties within a uniform DFT+DMFT scheme for these Hund's metals is missing. We show that the transport properties of these materials, especially their temperature dependence, are related to the underlying "resilient quasiparticles". We find that Sr_2RuO_4 is the least correlated one among the compounds considered, which corroborates its good metallicity.

We carry out the DFT+DMFT calculations with the all-electron DMFT as implemented in Ref. [35] based on Wien2K package[36]. The continuous-time quantum Monte-Carlo method with hybridization expansion is used to solve the impurity problem[37, 38]. A large energy window 20eV is used to construct the atomic-like localized d orbitals. This procedure permits us to use the same interaction parameters for all the ruthenates. We estimate the Slater integral within the localized orbitals assuming a screened Yukawa-form Coulomb potential $e^{-r/\lambda}/r$. With a proper choice of λ we have $(F^0, F^2, F^4) = (4.5, 8.0, 6.5)\text{eV}$, which amounts to $(U, J) = (4.5, 1.0)\text{eV}$. We note that in previous studies[9, 32, 33] smaller interaction parameters are used, because there the local orbitals are constructed in much smaller energy windows thus more extended. As shown below for all the compounds our current choice gives results in agreement with experiments and similar quasiparticle mass enhancements as in previous studies. The standard double counting in the fully localized limit form is adopted. The resistivity and optical conductivity are calculated using formalism of Ref.[35] in which the vertex corrections to the transport are neglected. Both polynomial fitting to the low frequency data and maximum entropy method are used to analytically continue

the computed self energy. We focus on the paramagnetic states only and neglect the ferromagnetism in SrRuO₃ at low temperature.

We first justify our choice of interaction parameters by examining the effective mass enhancement, which is computed by $m_{\text{theory}}^*/m_{\text{DFT}} = 1/Z = 1 - \frac{\partial \text{Re}\Sigma(\omega)}{\partial \omega}|_{\omega=0}$. These values extracted at $T = 58\text{K}$ are presented in Table.I, along with their experimental estimations. For CaRuO₃ and Sr₂RuO₄, they are in good agreement with experiments, and with previous DFT+DMFT calculations[9, 32, 33]. For SrRuO₃ no comparison is available since measurements are performed in the ferromagnetic state. Our result shows that the correlation strength of SrRuO₃ is close to the one of CaRuO₃ despite that the latter has a larger distortion and slightly narrower bandwidth. The correlation is stronger in the considered paramagnetic phase than that in the experimental ferromagnetic phase, which is generally expected since magnetism tends to reduce correlation. Sr₃Ru₂O₇ is peculiar where a strong momentum-dependence of the effective mass enhancement is revealed by high quality quantum oscillation (QO) and angular-resolved photoemission (ARPES) measurements [19, 24]. The strong momentum dependence is beyond our single-site DMFT approach. However our calculation gives a value very close to the mass enhancement (~ 6) on a large portion of the Fermi surface as found by ARPES [24]. Since the theoretical mass enhancements across all the materials agree reasonably well with available experimental values, the current choice of parameters is satisfactory. We note that Sr₂RuO₄ has smaller effective mass enhancements than its siblings, in agreement with experiments.

| | Sr ₂ RuO ₄ | Sr ₃ Ru ₂ O ₇ | SrRuO ₃ | CaRuO ₃ |
|---|----------------------------------|--|--------------------|--------------------|
| $m_{\text{theory}}^*/m_{\text{DFT}}$ | 4.3 (<i>xz/yz</i>) | 6.3 (<i>xz/yz</i>) | 6.6 | 6.7 |
| | 5.6 (<i>xy</i>) | 6.4 (<i>xy</i>) | | |
| $\gamma_{\text{exp}}/\gamma_{\text{DFT}}$ | 4 | 9 | 3.7 (FM) | 6.5 |
| $m_{\text{ARPES}}^*/m_{\text{DFT}}$ | $\simeq 3$ [21, 23] | $\simeq 6$ [24] | | |
| $m_{\text{QO}}^*/m_{\text{DFT}}$ | 3, 3.5 (<i>xz/yz</i>) | | | 6.1 [25] |
| | 5.5 (<i>xy</i>)[17] | | | |

TABLE I. The mass enhancement of ruthenates obtained in current DFT+DMFT calculations at $T = 58\text{K}$. Values estimated from specific heat coefficients, ARPES and quantum-oscillation measurements are presented for comparison. The experimental specific heat coefficients γ_{exp} are taken from Ref 12–16, while the corresponding DFT values are computed with Wien2K. $m_{\text{theory}}^*/m_{\text{DFT}}$ of SrRuO₃ and CaRuO₃ is averaged over t_{2g} orbitals. We note the $m_{\text{ARPES}}^*/m_{\text{DFT}}$ of Sr₃Ru₂O₇ is taken from a large fraction of the Fermi surface as discussed in the text. The $m_{\text{QO}}^*/m_{\text{DFT}}$ of CaRuO₃ is the value at zero magnetic field estimated from the data in Ref. 25 assuming Kadowaki-Woods relation.

The computed optical conductivities at room temperature are shown in Fig. 1 along with the experimental

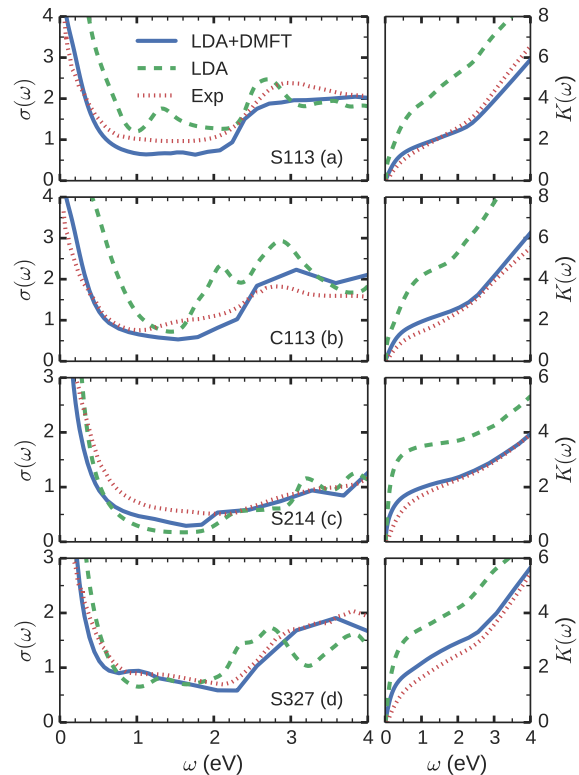


FIG. 1. The optical conductivity (left panel) and the corresponding integrated spectral weight (right panel) of ruthenates calculated within DFT+DMFT method ($T = 298\text{K}$) and DFT. Experimental data at room temperature are taken from 39 for comparison. S113, C113, S214, S327 are acronyms for SrRuO₃, CaRuO₃, Sr₂RuO₄ and Sr₃Ru₂O₇.

measurements and DFT results. Our calculated optical conductivities are consistent with the experiment measurements for all the compounds considered, and DMFT improves systematically the DFT results. The height and width of the Drude response are reasonably captured in our calculations. We note that the Drude response contains not only intra-orbital but also inter-orbital transition among t_{2g} orbitals, which is argued to be important for the $\omega^{-1/2}$ behavior in CaRuO₃ [33]. A broad peak centered around 3eV appears in all the compounds as observed in experiments. The broad peak is assigned to the transition between the O-2*p* to Ru-*d* orbitals. Note that DFT predicts an additional peak in SrRuO₃ at about 1.5eV and in CaRuO₃ at about 2.0eV, which can be assigned to t_{2g} - e_g transition. The amplitude of t_{2g} - e_g transition depends on the extent of GdFeO₃ distortion, and is insignificant or even missing in Sr₃Ru₂O₇ and Sr₂RuO₄, likely due to the matrix-element effects. However these peaks are shifted to higher frequency and merged with the broad peak at 3eV in our DFT+DMFT calculations in agreement with experiments.

The spectral weight distributions, computed as $K(\omega) = \int_0^\omega \sigma(\omega') d\omega'$, from both experimental and calcu-

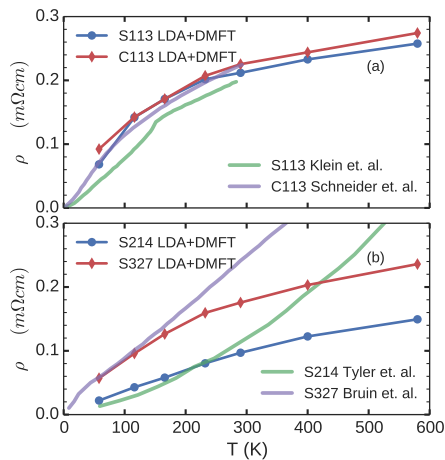


FIG. 2. The calculated resistivity of ruthenates with DFT+DMFT method for different temperature. The experimental measurements shown for for comparison are taken from 25, 28–30.

lated optical conductivities, are also depicted in Fig. 1. Strong correlations normally induce an anomalous spectral weight redistribution, which is the case in ruthenates. Compared with the DFT spectral weight distribution, a significant reduction is seen in the experimental data for all the ruthenates. A fraction of spectral weight is transferred to much higher frequency ($\geq 4eV$). The current DFT+DMFT calculations give spectral weight distributions in good agreements with experiments and capture the spectral weight reduction of LDA band theory nicely for all the compounds. The good agreements between theory and experiments of both optical conductivity and spectral weight distribution are solid evidences that electron-electron correlations dominate the electron dynamics in ruthenates.

Now we focus on the resistivity of these compounds which is directly related to zero-frequency limit of the optical response. The results are depicted in Fig.2 and compared with experiments. We note that in our calculations the resistivity of $SrRuO_3$ ($CaRuO_3$) has a relative small anisotropy (less than 15%), in accordance with experimental determinations[40, 41], therefore only its average over three principle axis is presented. For $CaRuO_3$ the agreement between the calculated and measured resistivity is almost perfect in both the overall scale and the temperature dependence in the whole temperature range. The shoulder at around 200K which marks the substantial change of the slope of the resistivity is well captured. For $SrRuO_3$ the calculated resistivity is very close to the one of $CaRuO_3$. Its agreement with experiment is very good above the Curie temperature $T_c \sim 160K$, however below T_c there is extra reduction of resistivity due to restoration of coherence in ferromagnetic state which is neglected in our calculations.

The agreement between the computed in-plane re-

sistivities of the layered compounds Sr_2RuO_4 and $Sr_3Ru_2O_7$ and the experiments as shown in Fig. 2(b), is not as good as for $CaRuO_3$. The calculated resistivities have similar temperature dependence as those of the pseudocubic compounds with a shoulder at around 200 ~ 300K. However the measured ones are different. The resistivity of $Sr_3Ru_2O_7$ is almost linear in temperature up to 300K with a weak shoulder showing up at low temperature (around 20K), and that of Sr_2RuO_4 does not exhibit a shoulder at all. Nevertheless there are three features correctly captured in our calculations. The resistivity of both compounds agree reasonably in the overall scale with experiments, especially at relative low temperature. The resistivity shows no sign of saturation at high temperature, although the increasing is not as fast as found in experiments. And going from pseudocubic structure to layered structure, the material becomes more conductive.

Despite the difference in the coherence scale, the computed resistivity of ruthenates where Hund's coupling dominates the correlations, has a very similar shape to the one of single band doped Hubbard model where Hubbard repulsion dominates the correlation[5]. Therefore this anomalous shape is likely a characteristic of the resistivity in single-site DMFT approach when the vertex corrections to the transport are neglected. Our results show that the vertex corrections are small in the pseudocubic ruthenate, but they are likely the cause of the discrepancy between this theory and experiments in layered compounds. Other effects such as electronic-phonon scattering and nonlocal interactions might also play some role.

We note that in agreement with experiments, both Sr_2RuO_4 and $Sr_3Ru_2O_7$ exhibit strong anisotropy in our LDA+DMFT calculations that the calculated out-of-plane resistivity is orders of magnitude larger than the in-plane one. The large anisotropy comes from the anisotropy of the plasma frequency which is captured by DFT[42] and also presents in DFT+DMFT.

The relatively good metallicity of the layered compounds Sr_2RuO_4 with respect to its siblings is captured in our calculations. To gain more understanding we recall that the dc conductivity can be written as $\sigma = (\omega_p^*)^2 \tau_{tr}^* / 4\pi$, where the effective plasma frequency ω_p^* and the effective scattering rate $1/\tau_{tr}^*$ can be extracted from the computed optical conductivity [43]. As shown in Fig. 3, there is strong temperature dependence of ω_p^* and $1/\tau_{tr}^*$ in all the compounds, which are characteristics of underlying "resilient quasiparticles"[43]. Interesting unlike that of V_2O_3 in our previous study, $(\omega_p^*)^2$ in ruthenates shows a saturation (or weak temperature dependence) above $T \simeq 200K$. This is possibly a characteristic of Hund's metal and needs to be justified in further studies. As discussed in Ref. 43, $(\omega_p^*)^2$ and $1/\tau_{tr}^*$ are directly related to $1/Z$ and the quasiparticle scattering rate $\Gamma^* = -2Z\text{Im}\Sigma(0)$, which have also strong

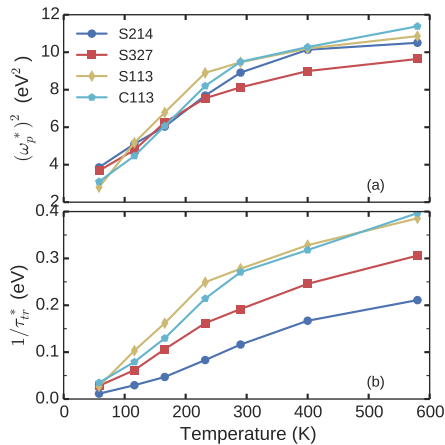


FIG. 3. The effective plasma frequency square $(\omega_p^*)^2$ and the effective quasiparticle scattering rate $1/\tau_{tr}^*$ extracted from the computed optical conductivity with DFT+DMFT method according to the formalism in Ref. 43.

temperature dependences as shown in Fig.4 for different orbitals. $1/Z$'s decreases when the temperature increases as found in previous study[5, 6, 43], and interestingly all approach approximately 2 at high temperature. The temperature dependence of $1/Z$ is consistent with that of effective optical mass inferred from THz conductivity of CaRuO₃[44]. In addition, we note both $1/\tau_{tr}^*$ and Γ^* generally show hidden Fermi liquid behavior at relative low temperature that they are approximately parabolic in temperature [6, 43], although the behavior is elusive in SrRuO₃.

Sr₂RuO₄ is the least correlated one in the ruthenates family according to the relative order of $1/\tau_{tr}^*$. To understand the relative correlation strength in ruthenates, we look into the orbital-resolved quantities, the low temperature effective mass enhancement $m_{\text{theory}}^*/m_{\text{DFT}}$ in Table.I and the quasiparticle scattering rate Γ^* in Fig. 4(b). We find that the $d_{xz/yz}$ orbitals in Sr₂RuO₄ are the special ones with significantly smaller $m_{\text{theory}}^*/m_{\text{DFT}}$ and Γ^* than the others. The uniqueness of $d_{xz/yz}$ orbitals in Sr₂RuO₄ can be traced back to their one-dimensional nature. Due to quantum confinement by Sr-O double-layer along out-of-plane axis, these orbitals have 1D singularities at their band edges, and a low density of states near the Fermi level with respect to the other orbitals. The relative weak correlation strength in these orbitals can be understood within the same argument of Ref.9, that the lower density of states ρ_F near the Fermi level implies stronger Weiss function in DMFT, $\text{Im}\Delta(\omega \rightarrow 0) \simeq -\frac{1}{\pi\rho_F}$, and results in weaker correlation. We note that this argument holds because in ruthenates the real part of the local Green's functions $\text{Re}G_{loc}(\omega)$ are much smaller than the imaginary part $\text{Im}G_{loc}(\omega) = -\pi\rho_F$ near Fermi level[45]. As n increases from Sr₂RuO₄ ($n = 1$), the density of states of $d_{xz/yz}$ orbitals near the Fermi level

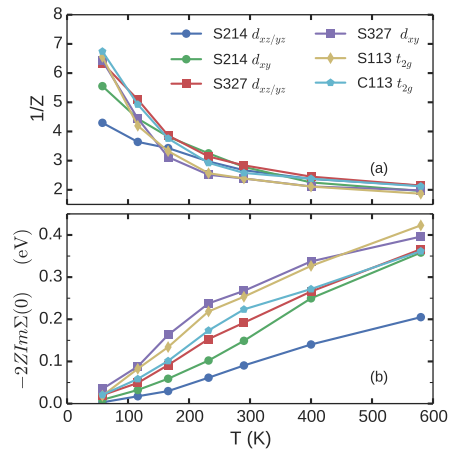


FIG. 4. The calculated effective mass enhancement $m_{\text{theory}}^*/m_{\text{DFT}} = 1/Z$ and the effective quasiparticle scattering rate $\Gamma^* = -2Z\text{Im}\Sigma(0)$ of different orbitals in ruthenates.

increases due to the relaxation of quantum confinement and the rotation of oxygen octahedra, therefore the correlation is enhanced. Meanwhile orbital differentiation is reduced so that eventually the $d_{xz/yz}$ orbitals become nearly degenerate with d_{xy} orbital in pseudocubic compounds thus exhibit similar correlations. However considering only d_{xy} orbitals (as well as $d_{xz/yz}$ orbitals in pseudocubic compounds due to the nearly degeneracy), we find that their Weiss functions do not correlate with their relative correlation strength. Rather the effective mass enhancement in these orbitals is mostly related to the in-plane Ru-O bond length and the rotation of oxygen octahedra[45]. The d_{xy} orbital in Sr₂RuO₄ is slightly less correlated than the others because of the short in-plane Ru-O bond length and the absence of oxygen octahedron rotations in this compound. Our findings may shed light on the correlation effects in ruthenate thin films and heterostructures where the quantum confinement[46], the Ru-O bond length and the distortions of oxygen octahedra could be engineered.

In conclusion, our DFT+DMFT calculations provide a quite accurate description of the transport properties in ruthenates. We demonstrate that the resilient quasiparticle scenario is valid beyond Hubbard-like repulsion in particular in Hund's metals. We explain the origin of the relative good metallicity in Sr₂RuO₄. Our results also suggests that effects such as vertex corrections, electron-phonon interactions or nonlocal interactions would need to be considered for more precise predictions of the resistivity of layered ruthenates.

We thank A. Georges and J. Mravlje for very useful discussions. We acknowledge supports by NSF DMR-1308141 (X. D. and G.K), NSF DMR 1405303 (K. H.).

Note: When preparing the manuscript we are aware of Ref.[34], which presents similar results on the temperature dependence of the effective mass enhancements in

SrRuO₃ and CaRuO₃ as in our study.

-
- [1] A. Georges, G. Kotliar, W. Krauth, and M. J. Rozenberg, *Reviews of Modern Physics* **68**, 13 (1996).
- [2] T. Pruschke, M. Jarrell, and J. K. Freericks, *Adv. Phys.* **44**, 187 (1995).
- [3] P. Nozières, *Theory Of Interacting Fermi Systems* (Addison-Wesley, Reading, MA, 1997).
- [4] V. J. Emery and S. A. Kivelson, *Physical Review Letters* **74**, 3253 (1995).
- [5] X. Deng, J. Mravlje, R. Žitko, M. Ferrero, G. Kotliar, and A. Georges, *Physical Review Letters* **110**, 086401 (2013).
- [6] W. Xu, K. Haule, and G. Kotliar, *Physical Review Letters* **111**, 036401 (2013).
- [7] K. Haule and G. Kotliar, *New Journal of Physics* **11**, 025021 (2009).
- [8] Z. P. Yin, K. Haule, and G. Kotliar, *Nature Physics* **7**, 294 (2011).
- [9] J. Mravlje, M. Aichhorn, T. Miyake, K. Haule, G. Kotliar, and A. Georges, *Physical Review Letters* **106**, 096401 (2011).
- [10] Z. P. Yin, K. Haule, and G. Kotliar, *Physical Review B* **86**, 195141 (2012).
- [11] A. Georges, L. d. Medici, and J. Mravlje, *Annual Review of Condensed Matter Physics* **4**, 137 (2013).
- [12] P. B. Allen, H. Berger, O. Chauvet, L. Forro, T. Jarlborg, A. Junod, B. Revaz, and G. Santi, *Physical Review B* **53**, 4393 (1996).
- [13] G. Cao, S. McCall, M. Shepard, J. E. Crow, and R. P. Guertin, *Physical Review B* **56**, 321 (1997).
- [14] M. Shepard, S. McCall, G. Cao, and J. E. Crow, *Journal of Applied Physics* **81**, 4978 (1997).
- [15] Y. Maeno, K. Yoshida, H. Hashimoto, S. Nishizaki, S.-i. Ikeda, M. Nohara, T. Fujita, A. P. Mackenzie, N. E. Hussey, J. G. Bednorz, and F. Lichtenberg, *Journal of the Physical Society of Japan* **66**, 1405 (1997).
- [16] S. Ikeda, Y. Maeno, S. Nakatsuji, M. Kosaka, and Y. Uwatoko, *Physical Review B* **62**, R6089 (2000).
- [17] C. Bergemann, A. P. Mackenzie, S. R. Julian, D. Forsythe, and E. Ohmichi, *Advances in Physics* **52**, 639 (2003).
- [18] C. S. Alexander, S. McCall, P. Schlottmann, J. E. Crow, and G. Cao, *Physical Review B* **72**, 024415 (2005).
- [19] A. Tamai, M. P. Allan, J. F. Mercure, W. Meevasana, R. Dunkel, D. H. Lu, R. S. Perry, A. P. Mackenzie, D. J. Singh, Z. Shen, and F. Baumberger, *Physical Review Letters* **101**, 026407 (2008).
- [20] J. Mercure, S. K. Goh, E. C. T. O’Farrell, R. S. Perry, M. L. Sutherland, A. W. Rost, S. A. Grigera, R. A. Borzi, P. Gegenwart, and A. P. Mackenzie, *Physical Review Letters* **103**, 176401 (2009).
- [21] H. Iwasawa, Y. Yoshida, I. Hase, K. Shimada, H. Namatame, M. Taniguchi, and Y. Aiura, *Physical Review Letters* **109**, 066404 (2012).
- [22] D. E. Shai, C. Adamo, D. W. Shen, C. M. Brooks, J. W. Harter, E. J. Monkman, B. Burganov, D. G. Schlom, and K. M. Shen, *Physical Review Letters* **110**, 087004 (2013).
- [23] C. N. Veenstra, Z. Zhu, B. Ludbrook, M. Capsoni, G. Levy, A. Nicolaou, J. A. Rosen, R. Comin, S. Kittaka, Y. Maeno, I. S. Elfimov, and A. Damascelli, *Physical Review Letters* **110**, 097004 (2013).
- [24] M. P. Allan, A. Tamai, E. Rozbicki, M. H. Fischer, J. Voss, P. D. C. King, W. Meevasana, S. Thirupathiah, E. Rienks, J. Fink, D. A. Tennant, R. S. Perry, J. F. Mercure, M. A. Wang, J. Lee, C. J. Fennie, E. Kim, M. J. Lawler, K. M. Shen, A. P. Mackenzie, Z. Shen, and F. Baumberger, *New Journal of Physics* **15**, 063029 (2013).
- [25] M. Schneider, D. Geiger, S. Esser, U. S. Pracht, C. Stingl, Y. Tokiwa, V. Moshnyaga, I. Sheikin, J. Mravlje, M. Scheffler, and P. Gegenwart, *Physical Review Letters* **112**, 206403 (2014).
- [26] G. Cao, W. Song, Y. Sun, and X. Lin, *Solid State Communications* **131**, 331 (2004).
- [27] N. E. Hussey, A. P. Mackenzie, J. R. Cooper, Y. Maeno, S. Nishizaki, and T. Fujita, *Physical Review B* **57**, 5505 (1998).
- [28] A. W. Tyler, A. P. Mackenzie, S. NishiZaki, and Y. Maeno, *Physical Review B* **58**, R10107 (1998).
- [29] J. a. N. Bruin, H. Sakai, R. S. Perry, and A. P. Mackenzie, *Science* **339**, 804 (2013), PMID: 23413351.
- [30] L. Klein, J. S. Dodge, C. H. Ahn, G. J. Snyder, T. H. Geballe, M. R. Beasley, and A. Kapitulnik, *Physical Review Letters* **77**, 2774 (1996).
- [31] G. Kotliar, S. Savrasov, K. Haule, V. Oudovenko, O. Parcollet, and C. Marianetti, *Reviews of Modern Physics* **78**, 865 (2006).
- [32] E. Jakobi, S. Kanungo, S. Sarkar, S. Schmitt, and T. Saha-Dasgupta, *Physical Review B* **83**, 041103 (2011).
- [33] H. T. Dang, J. Mravlje, A. Georges, and A. J. Millis, arXiv:1412.7803 [cond-mat] (2014), arXiv: 1412.7803.
- [34] H. T. Dang, J. Mravlje, A. Georges, and A. J. Millis, arXiv:1501.03964 [cond-mat] (2015), arXiv: 1501.03964.
- [35] K. Haule, C. Yee, and K. Kim, *Physical Review B* **81**, 195107 (2010).
- [36] P. Blaha, K. Schwarz, G. K. H. Madsen, D. Kvasnicka, and J. Luitz, *WIEN2K, An Augmented Plane Wave + Local Orbitals Program for Calculating Crystal Properties* (Karlheinz Schwarz, Techn. Universität Wien, Austria, Wien, Austria, 2001).
- [37] K. Haule, *Physical Review B* **75**, 155113 (2007).
- [38] P. Werner, A. Comanac, L. de’ Medici, M. Troyer, and A. J. Millis, *Physical Review Letters* **97**, 076405 (2006).
- [39] J. S. Lee, Y. S. Lee, T. W. Noh, S. Nakatsuji, H. Fukazawa, R. S. Perry, Y. Maeno, Y. Yoshida, S. I. Ikeda, J. Yu, and C. B. Eom, *Physical Review B* **70**, 085103 (2004).
- [40] I. Genish, L. Klein, J. W. Reiner, and M. R. Beasley, *Physical Review B* **75**, 125108 (2007).
- [41] D. L. Proffit, H. W. Jang, S. Lee, C. T. Nelson, X. Q. Pan, M. S. Rzechowski, and C. B. Eom, *Applied Physics Letters* **93**, 111912 (2008).
- [42] D. J. Singh, *Physical Review B* **52**, 1358 (1995).
- [43] X. Deng, A. Sternbach, K. Haule, D. N. Basov, and G. Kotliar, *Physical Review Letters* **113**, 246404 (2014).
- [44] S. Kamal, J. S. Dodge, D. Kim, and C. Eom (*Optical Society of America*, 2005) p. QWC2.
- [45] See Supplementary Materials at [url], for the Weiss function and the local Green’s functions for all the orbitals, as well as the relation of the correlation strength in d_{xy} orbital and the structure parameters.
- [46] Y. J. Chang, C. H. Kim, S. Phark, Y. S. Kim, J. Yu, and T. W. Noh, *Physical Review Letters* **103**, 057201 (2009).